Am J Cancer Res 2020;10(1):249-262
www.ajcr.us /ISSN:2156-6976/ajcr0104903

Original Article

Conditionally reprogrammed colorectal cancer cells combined with mouse avatars identify synergy between EGFR and MEK or CDK4/6 inhibitors

Yanni Wang[1*], Haiyan Liao[2*], Tongsen Zheng[3], Jingyuan Wang[1], Dagang Guo[4], Zhihao Lu[1], Zhongwu Li[5], Yiyou Chen[4], Lin Shen[1], Yanqiao Zhang[3], Jing Gao[2]

[1]Department of Gastrointestinal Oncology, Key Laboratory of Carcinogenesis and Translational Research (Ministry of Education/Beijing), Peking University Cancer Hospital and Institute, Beijing, China; [2]National Cancer Center/National Clinical Research Center for Cancer/Cancer Hospital & Shenzhen Hospital, Chinese Academy of Medical Sciences and Peking Union Medical College, Shenzhen 518116, China; [3]Department of Gastrointestinal Medical Oncology, Harbin Medical University Cancer Hospital, Harbin, China; [4]Percans Oncology, Beijing, China; [5]Department of Pathology, Key Laboratory of Carcinogenesis and Translational Research (Ministry of Education/Beijing), Peking University Cancer Hospital and Institute, Beijing, China. [*]Equal contributors.

Received November 14, 2019; Accepted December 6, 2019; Epub January 1, 2020; Published January 15, 2020

Abstract: Preclinical models, including patient-derived xenograft (PDX) and organoid and primary cell culture, are essential for studies of cancer cell biology and facilitate translational research and individualization of therapy. We explored the optimum preclinical model by modifying the conventional conditional reprogramming (CR) system followed by screening effective targeted drug combinations against colorectal cancer (CRC). By modifying the ingredients of the culture medium used in a conventional CR system, a novel individualized CR system (termed i-CR) was established. Tumor samples from CRC patients were collected and PDX models were derived followed by high-throughput i-CR drug screening and validation of the effective targeted drug combinations. The i-CR system selectively expanded tumor cells rather than normal epithelial cells and facilitated high-throughput drug screening when combined with high-content imaging and quantitative analysis of cell proliferation. Using inhibitors targeting multiple signaling pathways identified by high-throughput i-CR drug screening, we discovered that inhibition of the EGFR and MEK or CDK4/6 pathways exerted a synergistic inhibitory effect against CRC, and we noted supersynergistic effects when EGFR, MEK, and CDK4/6 inhibitors were used simultaneously. These data were validated using paired PDX models, which showed marked inhibition of tumor growth. The novel i-CR system combined with PDX models will enable individualization of therapy and drug discovery, and strategies combining EGFR, MEK, and CDK4/6 inhibitors warrant clinical validation.

Keywords: Conditional reprogramming, mouse avatar, EGFR inhibitor, MEK inhibitor, CDK4/6 inhibitor

Introduction

To achieve individualized cancer therapy, novel preclinical models that more closely reflect the genomic complexity of cancers are needed [1-3]. Functional drug testing by traditional primary cell culture of patient tumor tissue is subject to the proliferation bias of different cell clones, which can lead to inaccurate results [4]. Patient-derived xenograft (PDX) models and organoids are suitable surrogates for original tumors [5-7]. Compared to conventional primary cell culture, PDX models and organoids can mimic patient genotypes, maintain intra-tumor heterogeneity, and evaluate the response to cancer therapies [8, 9]. We established a primary tumor bank with various tissue types, including colorectal (CRC) and gastric cancers, but the cost and duration of the experiments and low throughput of the PDX models hindered achievement of treatment goals, especially for late-stage disease [10].

Recently, a novel primary cell culture technology, conditional reprogramming (CR), was reported by Liu and coworkers and allows expansion of primary epithelial cells *in vitro* with high efficiency [11-13]. The CR system can be used to expand normal and tumor cells from different tissues, including surgical specimens, biopsies,

and PDX tissues. Thus, CR technology may guide the individualization of cancer treatment [14-17]. A limitation of CR technology is its inability to distinguish between tumor and normal epithelial cells, as both proliferate well in the system [13]. Normal epithelial cells proliferate better under aerobic conditions, making it impractical to distinguish the effects of drugs on patient tumor and normal cells.

Based on the conventional CR system, to guide the individualization of therapy, here we report a modified individual CR system (termed i-CR), characterized by selective expansion of tumor cells from CRC patients *in vitro*. When combined with staining for EpCAM, EdU (5-ethynyl-2'-deoxyuridine), and Hoechst, followed by high-content imaging quantitative analysis, the i-CR system enables highly sensitive, accurate, and rapid evaluation of multiple therapeutic regimens directly from tumor tissues. We tested this system using a panel of approved inhibitors targeting multiple signaling pathways and found that simultaneous inhibition of the EGFR and MEK or CDK4/6 pathways exerted a synergistic inhibitory effect on CRC, and noted supersynergy when EGFR, MEK, and CDK4/6 inhibitors were used simultaneously. These data were validated in paired PDX models, which showed marked inhibition of tumor growth. The i-CR system together with a PDX model is useful for individualization of therapy and drug discovery, and strategies combining EGFR, MEK, and CDK4/6 inhibitors need to be validated in clinical practice.

Materials and methods

Patients and ethics approval

This study was approved by the Medical Ethics Committee of Peking University Cancer Hospital, and all specimens were collected from patients with written informed consent for their samples to be used in future studies. All animal experiments were performed under sterile conditions at the specified-pathogen-free facility of Peking University Cancer Hospital and in accordance with the National Institutes of Health guide for the care and use of laboratory animals.

Establishment of PDX models

The PDX model was established as in our previous report [6]. Briefly, 6-8-week-old female NOD/SCID mice (Beijing HFK Bio-Technology Co., Ltd., Beijing, China) were used. Tumor samples from patients were immediately transferred to tissue preservation solution (Percans Oncology, Cat# ZK-RUO-0101, Beijing, China) and sliced into small fragments. The mice were inoculated with the fragments subcutaneously on one flank to produce xenografts called passage-1 (P1). Serial xenografts at different passages were generated using the same procedure.

In vivo drug treatment

When tumors reached approximately 250-300 mm^3, the animals were randomly allocated into several groups of five mice each. The day of randomization was defined as study day 0. Tumor volume was expressed in mm^3 using the following formula: V (volume) = $(a \times b^2)/2$, where a and b are the long and short diameters of the tumor, respectively. The drugs and dosing regimens were as follows: Cetuximab, 1 mg per mouse, intraperitoneal injection, once a week for 3 weeks; Trametinib, 0.3 mg/kg, oral, once a day for 21 days; Palbociclib, 75 mg/kg, oral, once a day for 21 days; and Sorafenib, 50 mg/kg, oral, once a day for 2 weeks. Tumor suppression was expressed as tumor growth inhibition (TGI), which was calculated according to the formula: TGI (%) = (1 - (Ti - T0)/(Vi - V0)) × 100. Ti is the mean tumor volume of the treatment group on the measurement day; T0 is the mean tumor volume of the treatment group at D0; Vi is the mean tumor volume of the control group at the measurement day; and V0 is the tumor volume of the control group at D0.

Generation of patient-derived primary cultures (i-CR)

Swiss 3T3 fibroblasts (J2 strain) were purchased from The Cell Bank of the Type Culture Collection of the Chinese Academy of Sciences, Shanghai, China. The isolation and cultivation of i-CR primary tumor cells and normal primary epithelial cells were similar to the method of Liu *et al*., with modifications. Briefly, resected human tumor samples were quickly transferred into Roswell Park Memorial Institute (RPMI) 1640 medium containing 100 u/mL penicillin and 100 μg/mL streptomycin. Tissue samples were rinsed twice with cold phosphate-buffered saline (PBS), transferred to a sterile Petri dish, and minced using surgical scissors prior to enzymatic dissociation. The digestion enzymes

were collagenases, DNase, and dispase. Final cell suspensions were filtered through 100-μm cell strainers, followed by pelleting and resuspension in complete medium or selective medium. The complete medium consisted of DMEM/F-12 basal medium, 2% fetal bovine serum (FBS), 10 ng/mL human epithelial growth factor (EGF) (Thermo Fisher), 10 μM Y-27632 (Selleckchem), 10 ng/mL basic fibroblast growth factor (bFGF) (Thermo Fisher), 10 mM nicotinamide (Sigma), 1X insulin-transferrin-selenium (Thermo Fisher), 1X non-essential amino acids (Thermo Fisher), 25 ng/mL mouse Wnt3a (Peprotech), 500 ng/mL human R-spondin-1 (Peprotech), 100 ng/mL Noggin, and 100 μg/mL Primocin (Vivogen). The selective medium was complete medium lacking Wnt3a, R-spondin-1, and Noggin. Cells were seeded onto a feeder layer of lethally irradiated (40 Gy) Swiss 3T3 fibroblasts (J2 strain) feeder cells and incubated for approximately 1 week at 37°C in 5% CO_2.

Next-generation sequencing and data analysis

PDX tissues and paired i-CR cultures were analyzed for gene variations by targeted next-generation sequencing (NGS) of 483 genes. Genomic DNA extraction, library preparation, sequencing, and variants calling were performed as described previously [18].

Drug screening in i-CR cultures

Approximately 5,000 cells were seeded per well into a 96-well black-walled clear-bottom microplate (Corning), which was layered with feeder cells 24 h prior. The cells were cultured until small colonies were visible. All drugs (Table S1) were first dissolved in dimethyl sulfoxide (DMSO) as 1000X stocks and added to each well according to the study design. Typically, drugs were tested *in vitro* at the human steady-state serum concentration, or in serial dilutions when lower concentrations were needed. Cells were continuously treated for 7 days, with 1 μM EdU added for the final 24-48 h of incubation. Next, the cells were fixed and stained with EpCAM antibody, and the test plates were scanned using an Arrayscan XTI 800 (Thermo Scientific). Microscopic images were acquired and analyzed with the built-in Bioapplication software package. The effects of each treatment regimen were quantified using the formula: maximum inhibition (MI) = N0/Nd, where N0 and Nd denote the number of EdU- and EpCAM-positive epithelial cells in wells treated with DMSO control and drug, respectively. A combination index (CI) was modified from the Bliss Independence Model under an effect-based strategy to accommodate the drug effect ratio.

Inhibition percentage of drug A (AI) = 1 - EdU-positive cells in A treatment/EdU-positive cells in the control.

Inhibition percentage of drug AB (ABI) = 1 - EdU-positive cells in AB treatment/EdU-positive cells in the control.

Inhibition percentage of drug ABC (ABCI) = 1 - EdU-positive cells in ABC treatment/EdU-positive cells in the control.

The combination index (CI) was calculated as:

CI (AB) = (AI + BI - AI × BI)/(ABI).

CI (ABC) = (AI + BI + CI - AI × BI - AI × CI - BI × CI + AI × BI × CI)/(ABCI).

If CI < 1, the combination of A and B is synergistic.

If CI = 1, the combination of A and B is additive.

If CI > 1, the combination of A and B is antagonistic.

Statistical analysis

Statistical analysis was performed using Statistical Package for the Social Sciences (SPSS) ver. 20.0 or GraphPad Prism ver. 6.0 (GraphPad Software) software. Differences between groups were evaluated using the chi-squared test, unpaired two-tailed *t*-test, or one-way analysis of variance (ANOVA). For the *in vivo* study, tumor growth between groups was compared using repeated-measures ANOVA. A two-sided $P < 0.05$ was considered statistically significant.

Results

The i-CR system could effectively culture tumor cells from tumor tissues

Figure 1A shows that tumor cells could be expanded directly from surgical tissues, PDX tissues, and biopsies using the CR system. The

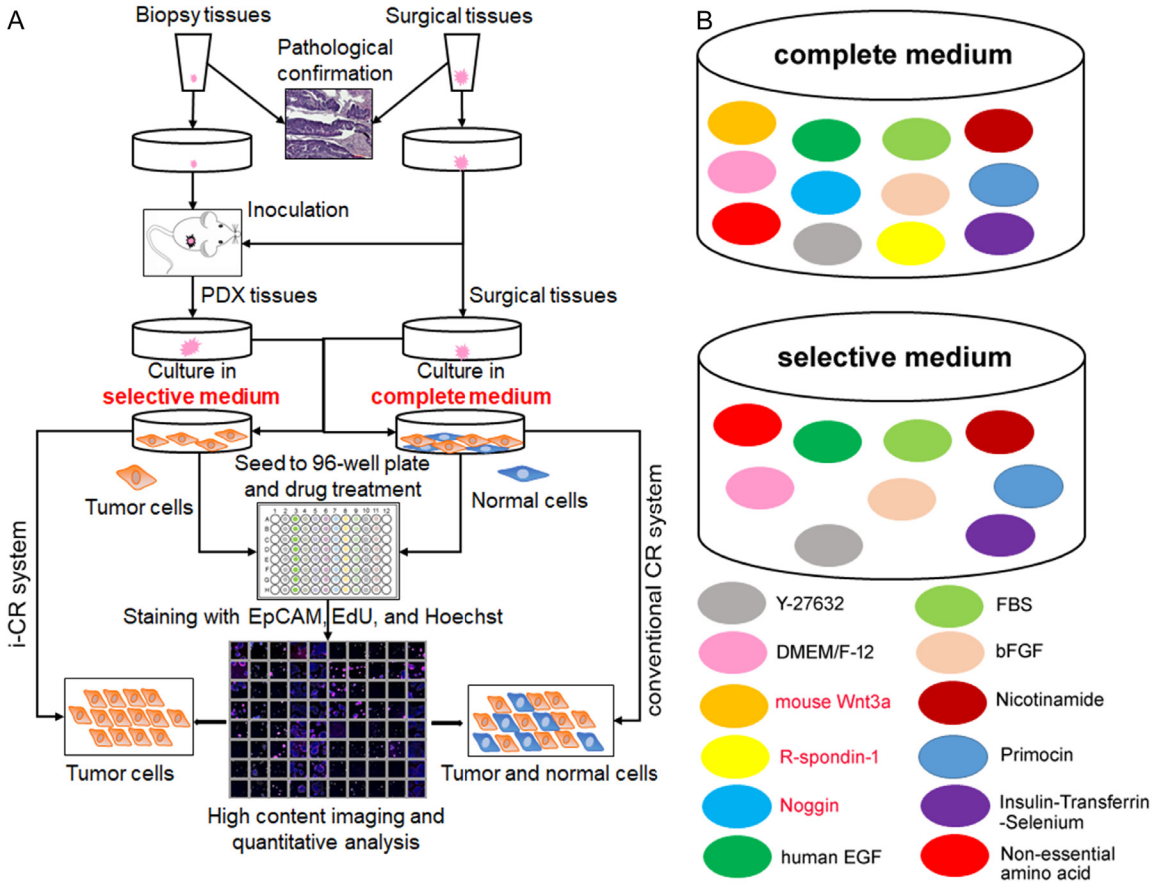

Figure 1. Schematic representation of a conventional CR system and the i-CR system. A. Pathologically confirmed surgical tumor tissues were collected and dissociated for *in vitro* drug treatment and analysis. Biopsy tissues were first inoculated into mice, and the PDX tumor tissues were collected and subjected to the same analytical process as surgical tumors. B. The major difference between the i-CR system and the conventional CR system is the composition of the cell-culture medium. Here, the selective medium was complete medium lacking Wnt 3A, R-spondin-1, and Noggin. Y-27632, ROCK1 inhibitor; FBS, fetal bovine serum; DMEM/F-12, Dulbecco's modified Eagle's medium/Ham's F-12 medium; bFGF, basic fibroblast growth factor; EGF, epidermal growth factor.

major difference between the i-CR system and a conventional CR system was the medium used (**Figure 1B**). In brief, to minimize the influence of normal epithelial cells on drug screens, we took advantage of the fact that the Wnt/β-catenin signaling pathway is adversely activated in more than 90% of CRC cases, while normal colonic epithelial cells are Wnt-dependent [13, 19]. Furthermore, BMP-related TGF-β signaling is downregulated in colon tumor cells, and suppression of this pathway may promote the proliferation of tumor cells but not normal colon cells. By removing the Wnt/β-catenin pathway activators Wnt 3A, R-spondin-1, as well as the BMP/TGFβ antagonist Noggin from the complete medium, we developed the selective medium. In general, for surgical tumor tissues, PDX models and i-CR cultures are carried out side by side. With regard to biopsy tissues, considering the small number of tumor cells, PDX models are preferred. If a PDX model was successfully established, the i-CR cells were cultured using the PDX tissues. To date, we have tested the i-CR culture system with > 300 CRC patient samples or PDX tumor samples. The overall success rate of i-CR culture was ~ 60% for surgical CRC tissues (~ 80% if contaminated samples were excluded) and > 90% for PDX tumor tissues. In total, 18 i-CR cultures from PDX tissues were used in the subsequent drug screening.

The i-CR system selectively expanded tumor cells rather than normal cells

In conventional CR systems, both tumor and normal cells from several tissues can be expanded. However, the growth conditions for

different tissue types can be improved. The i-CR system was optimized for the expansion of CRC epithelial cells. When compared with the conventional CR system, the i-CR system showed a notable advantage in terms of tumor cell proliferation with all CRC samples tested (number of EdU-positive cells) (**Figure 2A**).

Cells from normal colon or tumor tissues of the same patient were cultured in 96-well plates with complete medium or selective medium, respectively. As shown in **Figure 2B**, tumor cells rapidly proliferated in complete or selective medium; in contrast, normal epithelial cells proliferated in complete medium (green arrow) but failed to proliferate in selective medium. The quantitative results (**Figure 2C**) revealed that the number of EdU-positive normal cells in selective medium was less than 3% of that in complete medium, while the number of EdU-positive tumor cells in selective medium was more than 80% of that in complete medium. To analyze the effects of the modified culture conditions on tumor cells, we selected regions with a high tumor cell content from two patients' surgical colon tumor tissues and cultured each separately. As shown in **Figure 2D**, selective culture did not affect the growth or the phenotype of tumor cells.

As shown in **Figure 2E**, more than 95% of the tumor clones actively expanded in i-CR culture (**Figure 2E1**); in contrast, about 20% of the clones failed to proliferate in conventional cell culture within 3 days (**Figure 2E2**). This led us to speculate that the i-CR system maintains the proliferation of CRC tumor clones. Targeted next-generation sequencing (NGS) of 483 genes was performed in three PDX tissues (passage 3) and paired i-CR cells. As shown in **Figure 2F**, although a few inconsistent gene variations were observed between PDX tissues and paired i-CR cells, most genotypic profiling of i-CR cells revealed similarity to PDX tissues. In PDX-2 tissue and paired i-CR cells, for example, there were 16 and 12 gene variations, respectively, and 11 same-gene variations were detected in both PDX tissue and in paired i-CR cells. For PDX-3 tissue and paired i-CR cells, 12 same-gene variations were found, and for PDX-4 tissue and paired i-CR cells, 6 same-gene variations were found (**Figure 2F1** and **2F2**). The copy number of all tested genes was hardly changed (Table S2).

High-throughput screening of i-CR cultures revealed inhibitory synergy between the EGFR and MEK pathways or the EGFR and CDK4/6 pathways

Tumor cells expanded with the i-CR system were amenable to high-throughput drug screening, ranging from several to dozens of drugs or drug combinations. *In vitro* drug effects were analyzed using a highly sensitive method, providing detailed information for each treatment regimen (a representative example is shown in Figure S1). To identify potential therapies that could augment anti-EGFR therapy for CRC, we screened a panel of i-CR cultures with afatinib (a dual EGFR/HER2 inhibitor) plus a variety of targeted drugs (representative screening results are shown in Figure S2). As shown in **Figure 3A**, afatinib, the MEK inhibitor trametinib, or the CDK4/6 inhibitor palbociclib did not exert a strong tumor-suppressive effect, as indicated by a very low maximum inhibition (MI) when used alone. However, afatinib combined with trametinib or palbociclib exerted a significant synergistic effect in 12 of 13 i-CR cultures (combination index in Table S3). Interestingly, the combination of trametinib and palbociclib did not exhibit significant synergy.

Combinations of drugs targeting other pathways were also investigated for synergistic effects. No significant synergistic effects were observed for EGFR inhibitor/BRAF inhibitor, EGFR inhibitor/c-MET inhibitor, MEK inhibitor/BRAF inhibitor, or CDK4/6 inhibitor/BRAF inhibitor combinations (Table S3). To rule out the possibility that synergy was caused by off-target effects, or that the phenomenon was relevant only for specific compounds rather than signaling pathways, we tested multiple compounds targeting the EGFR, MEK, and CDK4/6 pathways in the same assay (**Figure 3A**). Similar synergistic effects were observed regardless of the compounds used, as long as relevant pathways were inhibited, suggesting that the synergies were pathway-specific rather than dependent on the drug molecule.

Interestingly, triple combinations of drugs targeting the EGFR, MEK, and CDK4/6 pathways had a markedly greater synergistic effect (super-synergy) compared with dual combinations, as indicated by significantly increased MI values (**Figure 3B**), suggesting super-synergy

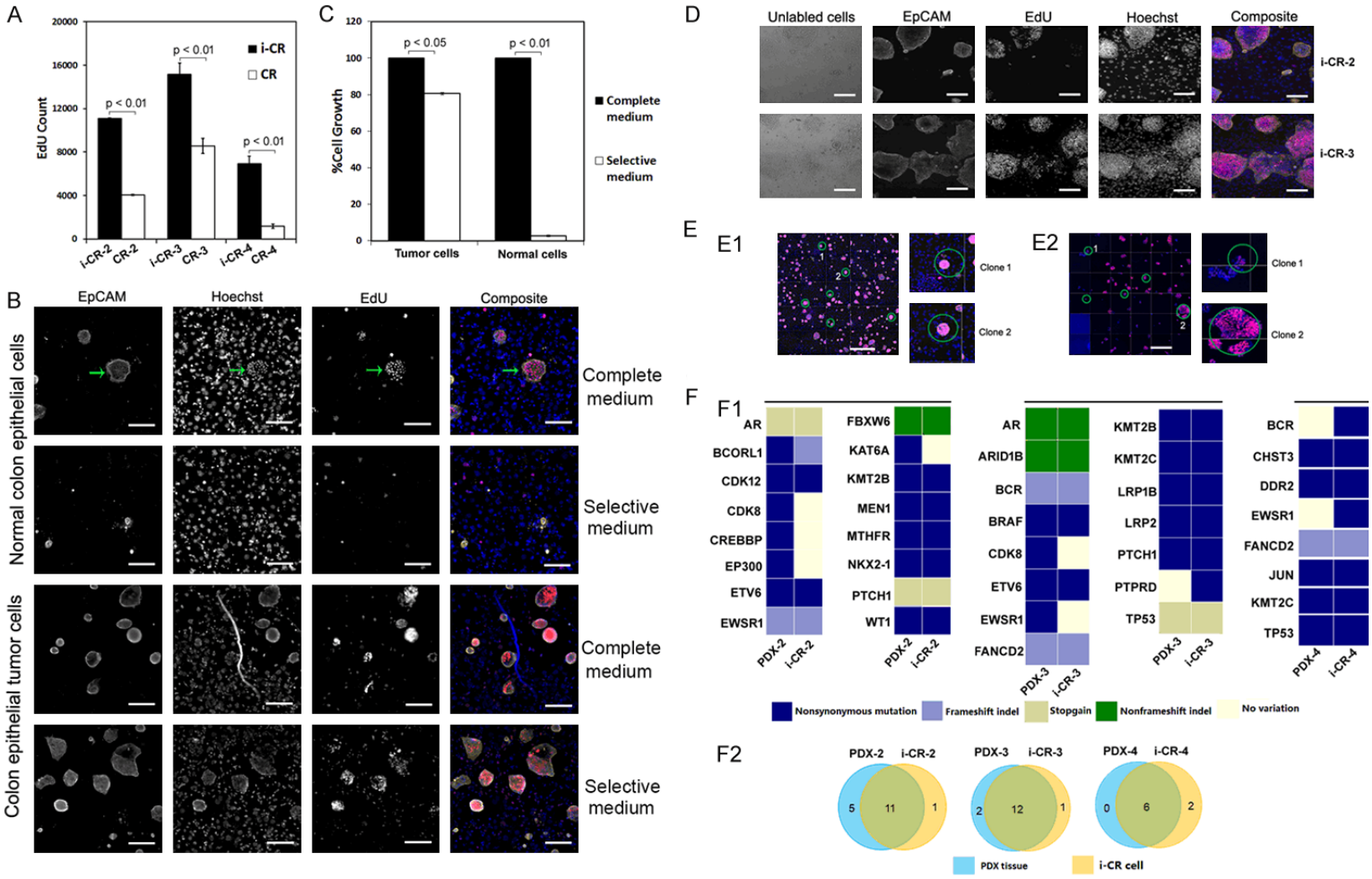

Figure 2. Development of the i-CR system and selective expansion of tumor cells from CRC patients. (A) Growth of tumor cells from CRC patients using the i-CR system and a conventional CR system. The number of EdU-positive cells cultured by the i-CR system was significantly greater than that by the conventional CR system in three patients. Experiments were performed in at least triplicate; $P < 0.01$. (B) Growth of tumor and normal cells in complete and selective medium. Proliferating normal cells (EdU-positive, red stain in the composite images) are indicated by green arrows. The cells were also stained with EpCAM (yellow) and Hoechst (blue). The scale bar equals 200 μm. (C) Quantitative analysis of cell growth in complete and selective medium. Data are averages of cells from three patient samples. Cell growth (number of EdU-positive cells) in complete medium was set as 100%. Normal epithelial cells failed to proliferate in selective medium, with the number of EdU-positive cells being less than 3% of that in complete medium ($P < 0.01$), compared to > 80% for tumor cells ($P < 0.05$). (D) High-content image analysis

of tumor cells grown in the presence of feeder cells. The scale bar equals 200 μm. (E) Preservation of tumor cell heterogeneity by the i-CR system or conventional cell culture. (E1) Denotes uniform clonal growth in i-CR culture and (E2) denotes loss of the proliferation of certain clones in conventional culture. The scale bar equals 1 mm. (F) Mutation profiles of PDX tissues and paired i-CR cells. (F1) Presents the variation genes for each PDX tissue and paired i-CR cells. Different color-coded blocks represent different variation types. (F2) Venn diagram of the number of variations for each PDX tissue and paired i-CR cells. Blue circle shows the variation number of PDX tissue and the yellow circle shows that of paired i-CR cells. The overlap in the middle represents the number of identical variations in PDX tissue and paired i-CR cells.

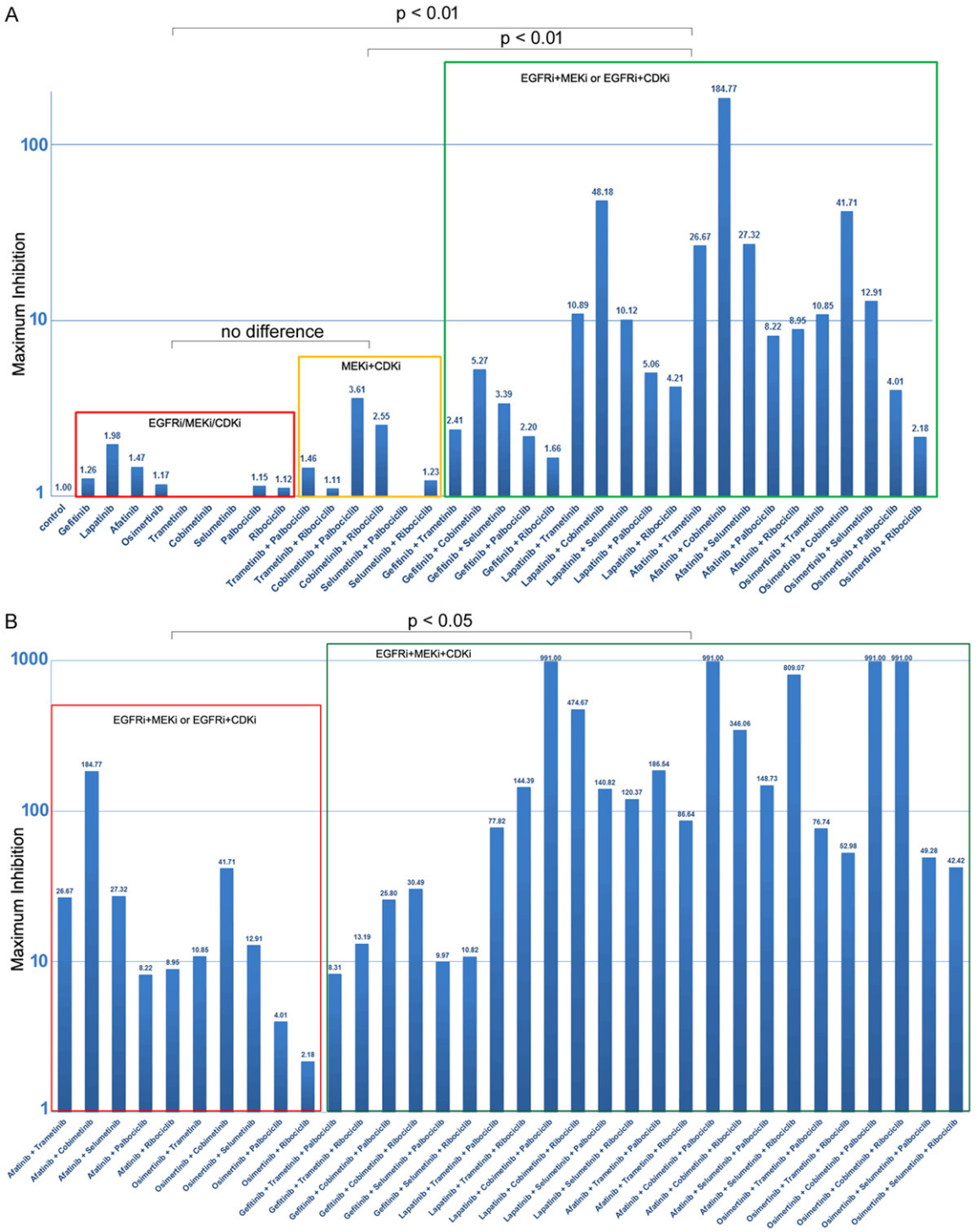

Figure 3. High-throughput screening of effective targeted therapy combinations for CRC patients. A. Synergistic effects of the EGFR and MEK or the EGFR and CDK4/6 pathways. The Y-axis denotes the maximum inhibition (MI), and the X-axis denotes the specific drugs or combinations used. Compared to any single drug (red box) or the MEKi/CDKi combination (orange box), EGFRi combined with MEKi or CDKi (green box) had a synergistic inhibitory effect; $P < 0.01$. B. Super-synergistic effect of triple pathway inhibition (green box) in comparison with dual pathway inhibition (red box). Data are expressed as means ± SEM of three independent experiments; $P < 0.05$. EGFRi, EGFR inhibitor; MEKi, inhibitor; CDKi, inhibitor.

instead of a mere additive effect. About 80% of the i-CR cultures responded strongly to triple combinations *in vitro* (Table S4). No such super-synergy was evident when drugs targeting BRAF were used in triple or even quadruple combinations (Table S4). Interestingly, in several cases, adding a BRAF inhibitor to the EGFR/MEK/CDK4/6 treatment led to weaker tumor growth inhibition than the triple combination (Table S4).

Validation of synergistic tumor suppression using EGFR/MEK/CDK4/6 inhibitors in paired PDX models

Next, we validated the *in vitro* screening results using paired PDX models *in vivo*. In one sample from a CRC patient with wild-type KRAS/NRAS/BRAF, a double or triple combination led to more growth inhibition *in vitro* than any single drug (MI values 8.22 [cetuximab + palbociclib], 26.67 [cetuximab + trametinib], and 186.54 [cetuximab + trametinib + palbociclib]) (**Figure 4A1**). The corresponding tumor growth inhibition (TGI) values in paired PDX models were 78.3%, 83.6%, and 95.2%, respectively (**Figure 4A2**). In a sample from another CRC patient with mutant KRAS (G12D), the triple combination yielded a higher MI value (79.16) than the single drugs (**Figure 4B1**). This was consistent with the *in vivo* data from the paired PDX model (TGI of 100.0%, **Figure 4B2**), suggesting that triple combinations exerted marked inhibition of tumors with wild-type and mutant RAS/RAF. Additional data from several CRC patients are listed in Table S5; the results obtained from *in vitro* tumor cells and *in vivo* PDX models were highly consistent.

The i-CR system enables assessment of drug-resistance mechanisms and predictive biomarkers

Clinical treatment response varies among patients, so there is an urgent need for biomarkers capable of distinguishing drug-sensitive from drug-resistant patients, as well as biomarkers that can predict treatment responses. As shown in Figure S3A, one i-CR culture from patient A was sensitive to 5-FU, while one from patient B was resistant. Consequently, we investigated predictive markers using omics and molecular biological methods. The i-CR system can easily identify resistant clones after drug treatments. Figure S3B presents one i-CR culture that contained both docetaxel-sensitive and -resistant clones. Because both clones had the same genetic background, it is feasible to sequence different clones to identify the mechanism underlying drug resistance. This warrants further exploration.

The persistence of proliferating clones after drug treatment is the driving force for tumor recurrence. **Figure 5A** shows that in one i-CR culture with KRAS mutation (G12V), the triple combination led to significant (MI 238, **Figure 5A1**) but partial tumor suppression, as evidenced by the persistence of drug-resistant clones in the culture after drug treatment. This is consistent with data from the paired PDX model, which revealed moderate inhibition of tumor growth (TGI 86.3%, **Figure 5A2**), and rapid tumor re-growth after drug withdrawal. In contrast, another i-CR culture (**Figure 5B**) with wild-type RAS/RAF revealed no detectable drug-resistant cells (MI of 5015, **Figure 5B1**) *in vitro* after triple-combination treatment, indicating that the frequency of drug-resistant tumor cells in this patient was less than $1/10^5$ (the upper limit of detection of the i-CR system). The paired PDX model revealed almost complete tumor suppression after drug treatment (**Figure 5B2**), and the suppression persisted long after drug withdrawal.

Discussion

Because few predictive biomarkers for chemotherapeutic sensitivity are available [20], the emergence of targeted therapy has changed the clinical landscape in oncology. With much lower toxicity and better clinical efficacy, many

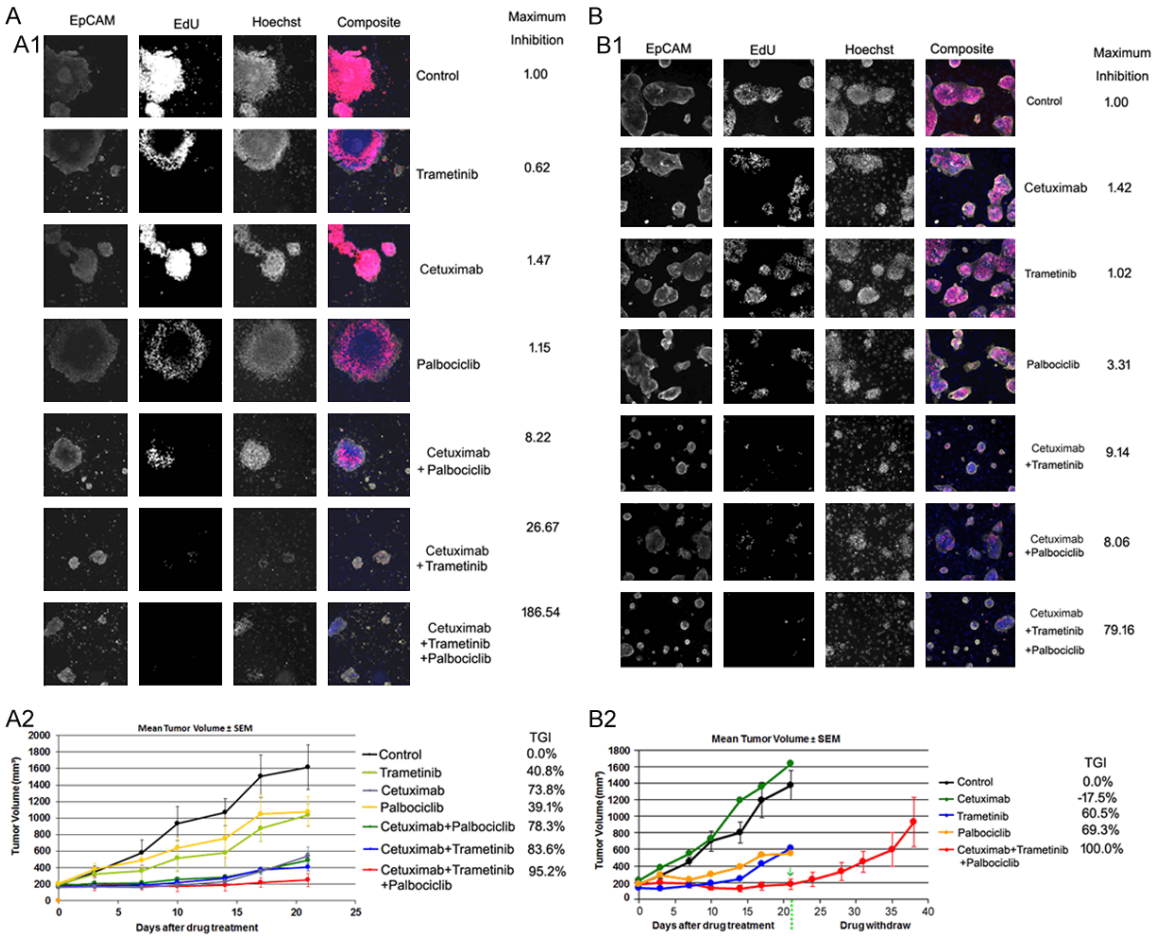

Figure 4. Synergistic effect of inhibition of EGFR and MEK or EGFR and CDK4/6. (A) Representative case of a correlation of tumor growth inhibition between the i-CR system (A1) and paired PDX models (A2). (B) Existence of residual drug-resistant clones in i-CR system (B1) predicts rapid tumor recurrence after drug withdrawal (green arrow shows the time of drug withdrawal) in PDX models (B2). Each microscopic frame represents a 0.976 × 0.976 mm view generated by the high-content screening (HCS) equipment. The cells were stained with EdU (red), EpCAM (yellow), and Hoechst (blue). Data are expressed as means ± SD of three independent experiments.

targeted drugs have been approved for clinical use for a variety of cancer types [21-27]. Clinical use of these drugs is often guided by specific genetic markers, for example, *HER2* overexpression or amplification for trastuzumab, and lack of *KRAS/NRAS/BRAF* gene mutation for cetuximab [21, 22]. However, the majority of cancer patients do not benefit from targeted therapies due to the absence of such genetic biomarkers, and some targeted drugs, such as bevacizumab and apatinib, lack this type of biomarker [24, 25]. Therefore, there is an urgent and increasing clinical need for a functional method of predicting the drug sensitivity of cancers.

Recently, PDX models have been used for translational oncology [8] because they mimic the tumor biology, including its genetic profile, clonal heterogeneity, and most importantly, therapeutic sensitivity [6, 9]. Despite these benefits, PDX models are limited by lack of growth *in vitro*, high cost, high labor-intensiveness, low throughput, and technical challenges. In recent years, CR technology, which is based on co-culture of epithelial cells with growth-arrested mouse 3 T3-J2 fibroblast feeders, has been used to achieve sustained expansion of human normal and tumor epithelial cells. To reduce the interference by normal cells with *in vitro* drug screening, we developed a novel CR system (i-CR) by removing the Wnt/β-catenin pathway activators Wnt 3A and R-spondin-1, and the BMP/TGFβ antagonist Noggin, from the complete medium used in the CR system. We explored the possibility of pre-

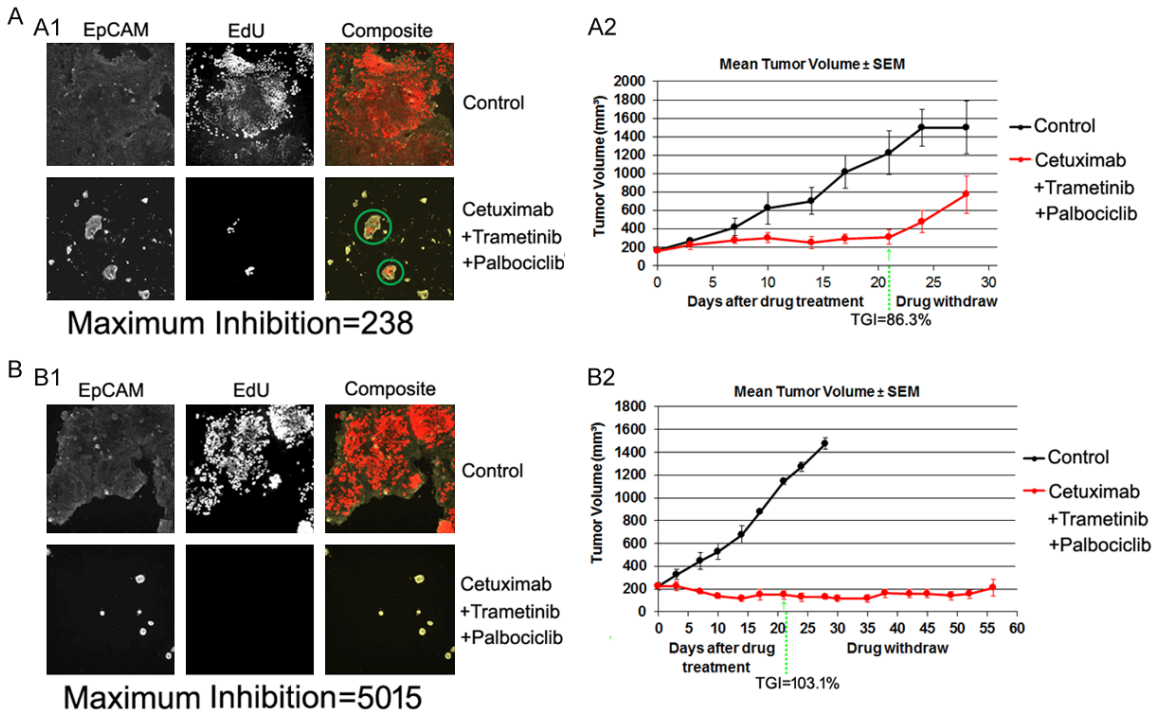

Figure 5. Use of the i-CR system to investigate drug-resistance mechanisms. (A) The existence of drug-resistant clones (green circle) (A1) with the triple combination regimen correlates with rapid tumor regrowth after drug withdrawal (green arrow shows the time of drug withdrawal) in paired PDX models (A2). (B) The complete absence of drug-resistant clones (B1) in culture correlates with profound tumor growth inhibition *in vivo* even after drug withdrawal (green arrow) (B2). Each frame represents a 0.976 × 0.976 mm view generated by the high-content screening (HCS) equipment.

dicting drug sensitivity using the i-CR system, especially when combined with PDX models. Compared to the conventional CR system reported by Liu and colleagues, the i-CR system represents a considerable improvement in three important respects. First, the i-CR system selectively expands primary CRC tumor cells while blocking the proliferation of normal epithelial cells. Surgical or biopsy tumor specimens often contain a large quantity of normal epithelial cells, which proliferate equally well as tumor cells in conventional CR systems, thus masking the real effects of drugs on tumor cells. Second, the majority of tumor cell clones proliferate well in the i-CR system. Third, the use of high-content imaging quantitative analysis provides sensitivity for single-cell detection and excludes signals from co-cultured tumor stromal cells that periodically grow in selective medium.

The i-CR system can rapidly screen many drugs or combinations *in vitro*, which can then be validated using paired PDX models *in vivo*. We have tested this system with a panel of targeted drugs in i-CR cultures. We observed significant synergy between inhibition of the EGFR and MEK pathways in both *KRAS/NRAS/BRAF* mutant and wild-type patients. Two clinical trials (NCT01750918, NCT01229150) of EGFR inhibitors and various MEK1/2 inhibitors have been initiated and include patients with mutations in the KRAS/BRAF pathway. Our data revealed that such a patient selection strategy might exclude some responsive patients who did not have the same mutation profile. We identified a synergistic effect of inhibition of the EGFR and CDK4/6 pathways. Inhibition of the EGFR and CDK4/6 pathways exerts a synergistic inhibitory effect on esophageal tumors [28], and this is the first report of such synergy against CRC. To confirm that this synergy is attributable to the pathways involved, rather than the specific drugs used in the assay, we tested inhibitors for each target. The same synergy was detected regardless of the drug or drug combination used. In contrast, such synergy did not exist between MEK and CDK4/6 inhibitors, EGFR and c-MET inhibitors, or EGFR and BRAF inhibitors. Anti-EGFR therapy represented by cetux-

imab is the mainstream treatment for CRC patients with wild-type *KRAS/NRAS/BRAF*, but it is often combined with other chemotherapy due to its weak single-agent efficacy. Our findings suggest directions for future clinical trials and support the use of a combination strategy targeting different signal transduction pathways [29, 30]. No synergistic effect of EGFR/HER2 inhibitors and BRAF inhibitors was found, and the mechanism underlying resistance to BRAF inhibitors is elusive. The mechanism is speculated to be as follows: BRAF is downregulated by feedback inhibition of ERK1/2 and inhibiting BRAF might not disrupt activation of the MEK-ERK1/2 pathway [31]; moreover, BRAF inhibition could adversely activate ERK1/2 signaling [32].

We found a super-synergistic tumor-suppressive effect when the EGFR, MEK, and CDK4/6 pathways were inhibited simultaneously in CRC tumor cells. In many cases, when dual inhibition of EGFR/MEK or EGFR/CDK4/6 exerted a synergistic effect compared to inhibition of either pathway alone, introduction of a third inhibitor resulted in additional synergy. More than 80% of our CRC cohorts responded to triple treatment, regardless of their *KRAS/NRAS/BRAF* genotype. We validated activity in paired PDX models in which no ROCK inhibitor was present, suggesting that EGFR, MEK, and CDK4/6 represent critical nodes for cancer cell growth regulation in CRC. This super-synergistic effect was also found in gastric and liver cancers (Figure S4), and additional efforts are ongoing to validate this observation with larger samples.

Our data were highly consistent between *in vitro* tumor cells and *in vivo* PDX models, and this strategy could also be used to investigate drug-resistance mechanisms and to identify predictive biomarkers. Most patients in clinical practice are treated without prior knowledge of their individual tumor cell biology, and the i-CR system may assist with patient triage in this regard. Moreover, the i-CR system can identify drug-resistant clones, the presence of which underlies tumor recurrence. DNA or RNA sequencing technologies can then be applied to determine the genetic mechanism of drug resistance. Using a similar approach, Crystal and colleagues identified drug combinations for lung cancer patients resistant to TKI [33], and Saeed and co-workers identified drugs that could be used to treat castration-resistant prostate cancer [34]. We have isolated clones resistant to specific treatment regimens and are investigating the mechanism of drug resistance.

We report here a novel i-CR system for the rapid expansion and functional screening of tumor cells from individual CRC patients, which has important implications for personalized therapy and drug discovery. The i-CR system has several advantages, including selective expansion of tumor cells, proliferation of almost all cell clones, single-cell detection sensitivity, and an up to 4-log dynamic range. Importantly, the whole procedure can be completed within 2-4 weeks, providing timely feedback for treatment decision-making. Interestingly, we also identified highly synergistic tumor-suppressive effects of the EGFR and MEK pathways and the EGFR and CDK4/6 pathways in CRC. EGFR/MEK/CDK triple inhibition exerted a super-synergistic effect, and we believe the combination of i-CR with PDX models to be a powerful new tool for individualization of therapy and for drug discovery.

Acknowledgements

We thank LetPub (www.letpub.com) for providing linguistic assistance during the preparation of this manuscript. This study was supported by the National Key Research and Development Program of China (No. 2017YFC1308900, 2017YFC0908400), and Beijing Municipal Administration of Hospital Clinical Medicine Development of Special Funding Support (ZYLX201701).

Disclosure of conflict of interest

None.

Address correspondence to: Jing Gao, National Cancer Center/National Clinical Research Center for Cancer/Cancer Hospital & Shenzhen Hospital, Chinese Academy of Medical Sciences and Peking Union Medical College, No. 113 Baohe Street, Longgang District, Shenzhen, China. Tel: +86-10-13581565966; E-mail: gaojing_pumc@163.com; Yanqiao Zhang, Department of Gastrointestinal Medical Oncology, Harbin Medical University Cancer Hospital, Harbin 150081, China. Tel: +86-451-86298222; Fax: +86-451-86298222; E-mail: yanqiaozhang@126.com

References

[1] Collins FS and Varmus H. A new initiative on precision medicine. N Engl J Med 2015; 372: 793-795.

[2] Friedman AA, Letai A, Fisher DE and Flaherty KT. Precision medicine for cancer with next-generation functional diagnostics. Nat Rev Cancer 2015; 15: 747-756.

[3] Serra-Musach J, Mateo F, Capdevila-Busquets E, de Garibay GR, Zhang X, Guha R, Thomas CJ, Grueso J, Villanueva A, Jaeger S, Heyn H, Vizoso M, Perez H, Cordero A, Gonzalez-Suarez E, Esteller M, Moreno-Bueno G, Tjarnberg A, Lazaro C, Serra V, Arribas J, Benson M, Gustafsson M, Ferrer M, Aloy P and Pujana MA. Cancer network activity associated with therapeutic response and synergism. Genome Med 2016; 8: 88.

[4] Schmitt MW, Loeb LA and Salk JJ. The influence of subclonal resistance mutations on targeted cancer therapy. Nat Rev Clin Oncol 2016; 13: 335-347.

[5] Bousquet G and Janin A. Patient-derived xenograft: an adjuvant technology for the treatment of metastatic disease. Pathobiology 2016; 83: 170-176.

[6] Zhu Y, Tian T, Li Z, Tang Z, Wang L, Wu J, Li Y, Dong B, Li Y, Li N, Zou J, Gao J and Shen L. Establishment and characterization of patient-derived tumor xenograft using gastroscopic biopsies in gastric cancer. Sci Rep 2015; 5: 8542.

[7] Vlachogiannis G, Hedayat S, Vatsiou A, Jamin Y, Fernandez-Mateos J, Khan K, Lampis A, Eason K, Huntingford I, Burke R, Rata M, Koh DM, Tunariu N, Collins D, Hulkki-Wilson S, Ragulan C, Spiteri I, Moorcraft SY, Chau I, Rao S, Watkins D, Fotiadis N, Bali M, Darvish-Damavandi M, Lote H, Eltahir Z, Smyth EC, Begum R, Clarke PA, Hahne JC, Dowsett M, de Bono J, Workman P, Sadanandam A, Fassan M, Sansom OJ, Eccles S, Starling N, Braconi C, Sottoriva A, Robinson SP, Cunningham D and Valeri N. Patient-derived organoids model treatment response of metastatic gastrointestinal cancers. Science 2018; 359: 920-926.

[8] Gao H, Korn JM, Ferretti S, Monahan JE, Wang Y, Singh M, Zhang C, Schnell C, Yang G, Zhang Y, Balbin OA, Barbe S, Cai H, Casey F, Chatterjee S, Chiang DY, Chuai S, Cogan SM, Collins SD, Dammassa E, Ebel N, Embry M, Green J, Kauffmann A, Kowal C, Leary RJ, Lehar J, Liang Y, Loo A, Lorenzana E, Robert McDonald E 3rd, McLaughlin ME, Merkin J, Meyer R, Naylor TL, Patawaran M, Reddy A, Roelli C, Ruddy DA, Salangsang F, Santacroce F, Singh AP, Tang Y, Tinetto W, Tobler S, Velazquez R, Venkatesan K, Von Arx F, Wang HQ, Wang Z, Wiesmann M, Wyss D, Xu F, Bitter H, Atadja P, Lees E, Hofmann F, Li E, Keen N, Cozens R, Jensen MR, Pryer NK, Williams JA and Sellers WR. High-throughput screening using patient-derived tumor xenografts to predict clinical trial drug response. Nat Med 2015; 21: 1318-1325.

[9] Roife D, Dai B, Kang Y, Perez MVR, Pratt M, Li X and Fleming JB. Ex vivo testing of patient-derived xenografts mirrors the clinical outcome of patients with pancreatic ductal adenocarcinoma. Clin Cancer Res 2016; 22: 6021-6030.

[10] Byrne AT, Alferez DG, Amant F, Annibali D, Arribas J, Biankin AV, Bruna A, Budinska E, Caldas C, Chang DK, Clarke RB, Clevers H, Coukos G, Dangles-Marie V, Eckhardt SG, Gonzalez-Suarez E, Hermans E, Hidalgo M, Jarzabek MA, de Jong S, Jonkers J, Kemper K, Lanfrancone L, Maelandsmo GM, Marangoni E, Marine JC, Medico E, Norum JH, Palmer HG, Peeper DS, Pelicci PG, Piris-Gimenez A, Roman-Roman S, Rueda OM, Seoane J, Serra V, Soucek L, Vanhecke D, Villanueva A, Vinolo E, Bertotti A and Trusolino L. Interrogating open issues in cancer precision medicine with patient-derived xenografts. Nat Rev Cancer 2017; 17: 254-268.

[11] Liu X, Krawczyk E, Suprynowicz FA, Palechor-Ceron N, Yuan H, Dakic A, Simic V, Zheng YL, Sripadhan P, Chen C, Lu J, Hou TW, Choudhury S, Kallakury B, Tang DG, Darling T, Thangapazham R, Timofeeva O, Dritschilo A, Randell SH, Albanese C, Agarwal S and Schlegel R. Conditional reprogramming and long-term expansion of normal and tumor cells from human biospecimens. Nat Protoc 2017; 12: 439-451.

[12] Liu X, Ory V, Chapman S, Yuan H, Albanese C, Kallakury B, Timofeeva OA, Nealon C, Dakic A, Simic V, Haddad BR, Rhim JS, Dritschilo A, Riegel A, McBride A and Schlegel R. ROCK inhibitor and feeder cells induce the conditional reprogramming of epithelial cells. Am J Pathol 2012; 180: 599-607.

[13] Palechor-Ceron N, Suprynowicz FA, Upadhyay G, Dakic A, Minas T, Simic V, Johnson M, Albanese C, Schlegel R and Liu X. Radiation induces diffusible feeder cell factor(s) that cooperate with ROCK inhibitor to conditionally reprogram and immortalize epithelial cells. Am J Pathol 2013; 183: 1862-1870.

[14] Agarwal S and Rimm DL. Making every cell like HeLa a giant step for cell culture. Am J Pathol 2012; 180: 443-445.

[15] Yuan H, Myers S, Wang J, Zhou D, Woo JA, Kallakury B, Ju A, Bazylewicz M, Carter YM, Albanese C, Grant N, Shad A, Dritschilo A, Liu X and Schlegel R. Use of reprogrammed cells to identify therapy for respiratory papillomatosis. N Engl J Med 2012; 367: 1220-1227.

[16] Beglyarova N, Banina E, Zhou Y, Mukhamadeeva R, Andrianov G, Bobrov E, Lysenko E, Skobeleva N, Gabitova L, Restifo D, Pressman M, Serebriiskii IG, Hoffman JP, Paz K, Behrens D, Khazak V, Jablonski SA, Golemis EA, Weiner LM and Astsaturov I. Screening of conditionally reprogrammed patient-derived carcinoma cells identifies ERCC3-MYC interactions as a target in pancreatic cancer. Clin Cancer Res 2016; 22: 6153-6163.

[17] Chia S, Low JL, Zhang X, Kwang XL, Chong FT, Sharma A, Bertrand D, Toh SY, Leong HS, Thangavelu MT, Hwang JSG, Lim KH, Skanthakumar T, Tan HK, Su Y, Hui Choo S, Hentze H, Tan IBH, Lezhava A, Tan P, Tan DSW, Periyasamy G, Koh JLY, Gopalakrishna Iyer N and Das-Gupta R. Phenotype-driven precision oncology as a guide for clinical decisions one patient at a time. Nat Commun 2017; 8: 435.

[18] Gao J, Wang H, Zang W, Li B, Rao G, Li L, Yu Y, Li Z, Dong B, Lu Z, Jiang Z and Shen L. Circulating tumor DNA functions as an alternative for tissue to overcome tumor heterogeneity in advanced gastric cancer. Cancer Sci 2017; 108: 1881-1887.

[19] van de Wetering M, Francies HE, Francis JM, Bounova G, Iorio F, Pronk A, van Houdt W, van Gorp J, Taylor-Weiner A, Kester L, McLaren-Douglas A, Blokker J, Jaksani S, Bartfeld S, Volckman R, van Sluis P, Li VS, Seepo S, Sekhar Pedamallu C, Cibulskis K, Carter SL, McKenna A, Lawrence MS, Lichtenstein L, Stewart C, Koster J, Versteeg R, van Oudenaarden A, Saez-Rodriguez J, Vries RG, Getz G, Wessels L, Stratton MR, McDermott U, Meyerson M, Garnett MJ and Clevers H. Prospective derivation of a living organoid biobank of colorectal cancer patients. Cell 2015; 161: 933-945.

[20] Uzilov AV, Ding W, Fink MY, Antipin Y, Brohl AS, Davis C, Lau CY, Pandya C, Shah H, Kasai Y, Powell J, Micchelli M, Castellanos R, Zhang Z, Linderman M, Kinoshita Y, Zweig M, Raustad K, Cheung K, Castillo D, Wooten M, Bourzgui I, Newman LC, Deikus G, Mathew B, Zhu J, Glicksberg BS, Moe AS, Liao J, Edelmann L, Dudley JT, Maki RG, Kasarskis A, Holcombe RF, Mahajan M, Hao K, Reva B, Longtine J, Starcevic D, Sebra R, Donovan MJ, Li S, Schadt EE and Chen R. Development and clinical application of an integrative genomic approach to personalized cancer therapy. Genome Med 2016; 8: 62.

[21] Bang YJ, Van Cutsem E, Feyereislova A, Chung HC, Shen L, Sawaki A, Lordick F, Ohtsu A, Omuro Y, Satoh T, Aprile G, Kulikov E, Hill J, Lehle M, Ruschoff J and Kang YK. Trastuzumab in combination with chemotherapy versus chemotherapy alone for treatment of HER2-positive advanced gastric or gastro-oesophageal junction cancer (ToGA): a phase 3, open-label, randomised controlled trial. Lancet 2010; 376: 687-697.

[22] Allegra CJ, Jessup JM, Somerfield MR, Hamilton SR, Hammond EH, Hayes DF, McAllister PK, Morton RF and Schilsky RL. American Society of Clinical Oncology provisional clinical opinion: testing for KRAS gene mutations in patients with metastatic colorectal carcinoma to predict response to anti-epidermal growth factor receptor monoclonal antibody therapy. J Clin Oncol 2009; 27: 2091-2096.

[23] Price TJ, Hardingham JE, Lee CK, Weickhardt A, Townsend AR, Wrin JW, Chua A, Shivasami A, Cummins MM, Murone C and Tebbutt NC. Impact of KRAS and BRAF gene mutation status on outcomes from the phase III AGITG MAX trial of capecitabine alone or in combination with bevacizumab and mitomycin in advanced colorectal cancer. J Clin Oncol 2011; 29: 2675-2682.

[24] Li J, Qin S, Xu J, Xiong J, Wu C, Bai Y, Liu W, Tong J, Liu Y, Xu R, Wang Z, Wang Q, Ouyang X, Yang Y, Ba Y, Liang J, Lin X, Luo D, Zheng R, Wang X, Sun G, Wang L, Zheng L, Guo H, Wu J, Xu N, Yang J, Zhang H, Cheng Y, Wang N, Chen L, Fan Z, Sun P and Yu H. Randomized, double-blind, placebo-controlled phase III trial of apatinib in patients with chemotherapy-refractory advanced or metastatic adenocarcinoma of the stomach or gastroesophageal junction. J Clin Oncol 2016; 34: 1448-1454.

[25] Keedy VL, Temin S, Somerfield MR, Beasley MB, Johnson DH, McShane LM, Milton DT, Strawn JR, Wakelee HA and Giaccone G. American Society of Clinical Oncology provisional clinical opinion: epidermal growth factor receptor (EGFR) Mutation testing for patients with advanced non-small-cell lung cancer considering first-line EGFR tyrosine kinase inhibitor therapy. J Clin Oncol 2011; 29: 2121-2127.

[26] Chapman PB, Hauschild A, Robert C, Haanen JB, Ascierto P, Larkin J, Dummer R, Garbe C, Testori A, Maio M, Hogg D, Lorigan P, Lebbe C, Jouary T, Schadendorf D, Ribas A, O'Day SJ, Sosman JA, Kirkwood JM, Eggermont AM, Dreno B, Nolop K, Li J, Nelson B, Hou J, Lee RJ, Flaherty KT and McArthur GA. Improved survival with vemurafenib in melanoma with BRAF V600E mutation. N Engl J Med 2011; 364: 2507-2516.

[27] Pujade-Lauraine E, Ledermann JA, Selle F, Gebski V, Penson RT, Oza AM, Korach J, Huzarski T, Poveda A, Pignata S, Friedlander M, Colombo N, Harter P, Fujiwara K, Ray-Coquard I, Banerjee S, Liu J, Lowe ES, Bloomfield R and Pautier P. Olaparib tablets as maintenance therapy in patients with platinum-sensitive, relapsed ovarian cancer and a BRCA1/2 muta-

tion (SOLO2/ENGOT-Ov21): a double-blind, randomised, placebo-controlled, phase 3 trial. Lancet Oncol 2017; 18: 1274-1284.

[28] Zhou J, Wu Z, Wong G, Pectasides E, Nagaraja A, Stachler M, Zhang H, Chen T, Zhang H, Liu JB, Xu X, Sicinska E, Sanchez-Vega F, Rustgi AK, Diehl JA, Wong KK and Bass AJ. CDK4/6 or MAPK blockade enhances efficacy of EGFR inhibition in oesophageal squamous cell carcinoma. Nat Commun 2017; 8: 13897.

[29] Li F, Zhao C and Wang L. Molecular-targeted agents combination therapy for cancer: developments and potentials. Int J Cancer 2014; 134: 1257-1269.

[30] Sharma P and Allison JP. Immune checkpoint targeting in cancer therapy: toward combination strategies with curative potential. Cell 2015; 161: 205-214.

[31] Hernandez MA, Patel B, Hey F, Giblett S, Davis H and Pritchard C. Regulation of BRAF protein stability by a negative feedback loop involving the MEK-ERK pathway but not the FBXW7 tumour suppressor. Cell Signal 2016; 28: 561-571.

[32] Poulikakos PI, Zhang C, Bollag G, Shokat KM and Rosen N. RAF inhibitors transactivate RAF dimers and ERK signalling in cells with wild-type BRAF. Nature 2010; 464: 427-430.

[33] Crystal AS, Shaw AT, Sequist LV, Friboulet L, Niederst MJ, Lockerman EL, Frias RL, Gainor JF, Amzallag A, Greninger P, Lee D, Kalsy A, Gomez-Caraballo M, Elamine L, Howe E, Hur W, Lifshits E, Robinson HE, Katayama R, Faber AC, Awad MM, Ramaswamy S, Mino-Kenudson M, Iafrate AJ, Benes CH and Engelman JA. Patient-derived models of acquired resistance can identify effective drug combinations for cancer. Science 2014; 346: 1480-1486.

[34] Saeed K, Rahkama V, Eldfors S, Bychkov D, Mpindi JP, Yadav B, Paavolainen L, Aittokallio T, Heckman C, Wennerberg K, Peehl DM, Horvath P, Mirtti T, Rannikko A, Kallioniemi O, Ostling P and Af Hallstrom TM. Comprehensive drug testing of patient-derived conditionally reprogrammed cells from castration-resistant prostate cancer. Eur Urol 2017; 71: 319-327.

Table S1. Drugs used *in vitro* drug screening

Drugs	Types	Concentration	Vendor
Gefitinib	EGFR inhibitor	2 μM	Meilunbio
Lapatinib	EGFR inhibitor	5 μM	Pharmacodia
Afatinib	EGFR inhibitor	0.1 μM	Meilunbio
Osimertinib	EGFR inhibitor	0.5 μM	Pharmacodia
Trametinib	MEK inhibitor	0.01 μM	Pharmacodia
Cobimetinib	MEK inhibitor	0.2 μM	Pharmacodia
Palbociclib	CDK inhibitor	1 μM	Pharmacodia
Ribociclib	CDK inhibitor	5 μM	Meilunbio
Dabrafenib	BRAF inhibitor	1 μM	Meilunbio
Crizotinib	MET inhibitor	0.25 μM	Meilunbio
5-FU	chemotherapy	10 μM	Pharmacodia
Docetaxel	chemotherapy	0.005 μM	Selleckchem

Table S2. Copy number of 483 genes

Gene	Copy number of i-CR-2	Copy number of PDX-2	Copy number of i-CR-3	Copy number of PDX-3	Copy number of i-CR-4	Copy number of PDX-4
RARA	2	2	2	2	2	2
ABCB1	2.86	2.72	2	2	2	2
ABCC1	2	2	2	2	2	2
ABCC2	2	2	2	2	2	2
ABCC4	2	2	2	2	4.86	4.58
ABCC6	2	2	2	2	2	2
ABCG2	2	2	2	2	2	2
ABL1	3.12	3.3	2	2	2	2
ACK1	2	2	2	2	2	2
ACVR1B	2	2	2	2	2	2
AKT1	2	2	2	2	2	2
AKT2	2	2	2	2	2	2
AKT3	2	2	2	2	2	2
ALK	2	2	2	2	2	2
AMER1	2	2	2	2	2	2
APC	2	2	2	2	2	2
AR	2	2	2	2	2	2
ARAF	2	2	2	2	2	2
ARFRP1	2	2	2	2	3.78	4.66
ARID1A	2	2	2	2	2	2
ARID1B	2	2	2	2	2	2
ARID2	2	2	2	2	2	2
ASXL1	2	2	2	2	4.82	4.8
ATIC	2	2	2	2	2	2
ATM	2	2	2	2	2	2
ATP7A	2	2	2	2	2	2
ATR	2	2	2	2	2	2
ATRX	2	2	2	2	2	2
AURKA	2	2	2	2	4.54	4.72
AURKB	2	2	2	2	2	2

AXIN1	2	2	2	2	2	2
AXL	2	2	2	2	2	2
B2M	2	2	2	2	2	2
BAIAP3	2	2	2	2	2	2
BAP1	2	2	2	2	2	2
BARD1	2	2	2	2	2	2
BCL2	2	2	2	2	2	2
BCL2L2	2	2	2	2	2	2
BCL6	2	2	2	2	2	2
BCOR	2	2	2	2	2	2
BCORL1	2	2	2	2	2	2
BCR	2	2	2	2	2	2
BIRC5	2	2	2	2	2	2
BLK	2	2	2	2	2	2
BLM	2	2	2	2	2	2
BRAF	2.78	2.64	2	2	2	2
BRCA1	2	2	2	2	2	2
BRCA2	2	2	2	2	4.68	3.8
BRIP1	2	2	2	2	2	2
BRK	2	2	2	2	2	2
BSG	2	2	2	2	2	2
BTK	2	2	2	2	2	2
C11orf30	2	2	2	2	2	2
C18orf56	2	2	2	2	2	2
C8orf34	2	2	4.02	3.46	2	2
CAMK2G	2	2	2	2	2	2
CAMKK2	2	2	2	2	2	2
CARD11	2.9	2.52	2	2	3.74	4.04
CASP8	2	2	2	2	2	2
CBFB	2	2	2	2	2	2
CBL	2	2	2	2	2	2
CBR1	2	2	2	2	2	2
CBR3	2	2	2	2	2	2
CCND1	2	2	2	2	2	2
CCND2	2	2	2	2	4.02	3.44
CCND3	2	2	2	2	2	2
CCNE1	2	2	2	2	2	2
CCR4	2	2	2	2	2	2
CD19	2	2	2	2	2	2
CD22	2	2	2	2	2	2
CD274	2.82	2.94	2	2	2	2
CD33	2	2	2	2	2	2
CD38	2	2	2	2	2	2
CD3EAP	2	2	2	2	2	2
CD52	2	2	2	2	2	2
CD74	2	2	2	2	2	2
CD79A	2	2	2	2	2	2
CD79B	2	2	2	2	2	2
CDA	2	2	2	2	2	2
CDC73	2	2	2	2	2	2

CDH1	2	2	2	2	2	2
CDK1	2	2	2	2	2	2
CDK12	2	2	2	2	3	3.36
CDK2	2	2	2	2	2	2
CDK4	2	2	2	2	2	2
CDK5	3.16	3.42	2	2	3.18	3.34
CDK6	3.18	3.4	2	2	2	2
CDK7	2	2	2	2	2	2
CDK8	2	2	2	2	2	2
CDK9	2.92	3.32	2	2	2	2
CDKN1B	2	2	2	2	3.76	3.84
CDKN2A	2	2	2	2	2	2
CDKN2B	2	2	2	2	2	2
CDKN2C	2	2	2	2	2	2
CEBPA	2	2	2	2	2	2
CHEK1	2	2	2	2	2	2
CHEK2	2	2	2	2	2	2
CHST3	2	2	2	2	2	2
CIC	2	2	2	2	2	2
COMT	2	2	2	2	2	2
CREBBP	2	2	2	2	2	2
CRKL	2	2	2	2	2	2
CRLF2	2	2	2	2	2	2
CSF1R	2	2	2	2	2	2
CSK	2	2	2	2	2	2
CSNK1A1	2	2	2	2	2	2
CTCF	2	2	2	2	2	2
CTLA4	2	2	2	2	4.28	3.36
CTNNA1	2	2	2	2	2	2
CTNNB1	2	2	2	2	2	2
CYBA	2	2	2	2	2	2
CYLD	2	2	2	2	2	2
CYP19A1	2	2	2	2	2	2
CYP1A1	2	2	2	2	2	2
CYP1A2	2	2	2	2	2	2
CYP1B1	2	2	2	2	2	2
CYP2A6	2	2	2	2	2	2
CYP2B6	2	2	2	2	2	2
CYP2C19	2	2	2	2	2	2
CYP2C8	2	2	2	2	2	2
CYP2C9	2	2	2	2	2	2
CYP2D6	2	2	2	2	2	2
CYP2E1	2	2	2	2	2	2
CYP3A4	2	2	2	2	2	2
CYP3A5	3.06	2.7	2	2	2	2
CYP4B1	2	2	2	2	2	2
DAXX	2	2	2	2	2	2
DDR1	2	2	2	2	2	2
DDR2	2.64	2.58	2	2	2	2
DNMT1	2	2	2	2	2	2

DNMT3A	2	2	2	2	2	2
DOT1L	2	2	2	2	2	2
DPYD	2	2	2	2	2	2
DSCAM	2	2	2	2	2	2
E2F1	2	2	2	2	4.38	4.88
EGF	2	2	2	2	2	2
EGFL7	2	2	2	2	2	2
EGFR	3	2.84	2	2	4.64	4.22
EGR1	2	2	2	2	2	2
EMC8	2	2	2	2	2	2
EML4	2	2	2	2	2	2
ENOSF1	2	2	2	2	2	2
EP300	2	2	2	2	2	2
EPHA1	3.2	2.82	2	2	2	2
EPHA2	2	2	2	2	2	2
EPHA3	2	2	2	2	2	2
EPHA4	2	2	2	2	2	2
EPHA5	2	2	2	2	2	2
EPHA7	2	2	2	2	2	2
EPHA8	2	2	2	2	2	2
EPHB1	2	2	2	2	2	2
EPHB2	2	2	2	2	2	2
EPHB3	2	2	2	2	2	2
EPHX1	2	2	2	2	2	2
ERBB2	2	2	2	2	3.18	3.56
ERBB3	2	2	2	2	2	2
ERBB4	2	2	2	2	2	2
ERCC1	2	2	2	2	2	2
ERCC2	2	2	2	2	2	2
ERG	2	2	2	2	2	2
ESR1	2	2	2	2	2	2
ETV1	2.52	2.68	2	2	4.42	3.56
ETV4	2	2	2	2	2	2
ETV5	2	2	2	2	2	2
ETV6	2	2	2	2	2	2
EWSR1	2	2	2	2	2	2
EZH2	2.98	2.94	2	2	2	2
FAM46C	2	2	2	2	2	2
FANCA	2	2	2	2	2	2
FANCC	3.02	3.1	2	2	2	2
FANCD2	2	2	2	2	2	2
FANCE	2	2	2	2	2	2
FANCF	2	2	2	2	2	2
FANCG	3.1	2.94	2	2	2	2
FANCL	2	2	2	2	2	2
FBXW7	2	2	2	2	2	2
FCGR3A	2	2	2	2	2	2
FGF10	2	2	4.76	4.58	2	2
FGF14	2	2	2	2	5.32	4.38

FGF19	2	2	2	2	2	2
FGF23	2	2	2	2	3.38	3.26
FGF3	2	2	2	2	2	2
FGF4	2	2	2	2	2	2
FGF6	2	2	2	2	3.22	3.52
FGFR1	2	2	4.2	3.7	2	2
FGFR2	2	2	2	2	2	2
FGFR3	2	2	2	2	2	2
FGFR4	2	2	2	2	2	2
FGR	2	2	2	2	2	2
FKBP1A	2	2	2	2	2	2
FLT1	2	2	2	2	4.4	3.92
FLT3	2	2	2	2	2	2
FLT4	2	2	2	2	2	2
FOXL2	2	2	2	2	2	2
FRK	2	2	2	2	2.52	3.6
FUBP1	2	2	2	2	2	2
FYN	2	2	2	2	2	2
FZD7	2	2	2	2	2	2
GALNT14	2	2	2	2	2	2
GATA1	2	2	2	2	2	2
GATA2	2	2	2	2	2	2
GATA3	2	2	2	2	2	2
GCK	2	2	2	2	3.84	3.92
GID4	2	2	2	2	2	2
GINS2	2	2	2	2	2	2
GNA11	2	2	2	2	2	2
GNA13	2	2	2	2	2	2
GNAQ	3	2.9	2	2	2	2
GNAS	2	2	2	2	5.12	5.04
GPC3	2	2	2	2	2	2
GPR124	2	2	3.84	3.34	2	2
GRIN2A	2	2	2	2	2	2
GSK3B	2	2	2	2	2	2
GSTM1	2	2	2	2	2	2
GSTM3	2	2	2	2	2	2
GSTP1	2	2	2	2	2	2
GSTT1	2	2	2	2	2	2
H3F3A	2	2	2	2	2	2
HCK	2	2	2	2	4.44	5.02
HGF	2	2	2	2	2	2
HIF1A	2	2	2	2	2	2
HIST1H3B	2	2	2	2	2	2
HNF1A	2	2	2	2	2	2
HRAS	2	2	2	2	3.26	3.48
HSP90AA1	2	2	2	2	2	2
IDH1	2	2	2	2	2	2
IDH2	2	2	2	2	2	2
IGF1	2	2	2	2	2	2

IGF2	2.64	2.8	2	2	3.86	3.64
IGF2R	2	2	2	2	2	2
IGFR	2	2	2	2	2	2
IKBKB	2	2	2	2	2	2
IKBKE	2	2	2	2	3.28	3.14
IKZF1	3.04	3.32	2	2	5.36	4.58
IL7R	2	2	4.76	5.02	2	2
INHBA	2.74	2.88	2	2	4.6	3.76
INSR	2	2	2	2	2	2
IRF4	2	2	2	2	2	2
IRS2	2	2	2	2	2	2
ITK	2	2	2	2	2	2
JAK1	2	2	2	2	2	2
JAK2	2.78	2.92	2	2	2	2
JAK3	2	2	2	2	2	2
JUN	2	2	2	2	2	2
KAT6A	2.56	2	2	2	2	2
KDM5A	2	2	2	2	2.7	3.04
KDM5C	2	2	2	2	2	2
KDM6A	2	2	2	2	2	2
KDR	2	2	2	2	2	2
KEAP1	2	2	2	2	2	2
KIT	2	2	2	2	2	2
KITLG	2	2	2	2	2	2
KLC3	2	2	2	2	2	2
KLHL6	2	2	2	2	2	2
KRAS	2	2	2	2	2	2
LCK	2	2	2	2	2	2
LIMK1	2.8	2.58	2	2	2	2
LMO1	2	2	2	2	3.48	3.26
LRP1B	2	2	2	2	2	2
LRP2	2	2	2	2	2	2
LYN	2	2	4.64	4.04	2	2
MAP2K1	2	2	2	2	2	2
MAP2K2	2	2	2	2	2	2
MAP2K4	2	2	2	2	2	2
MAP3K1	2	2	2	2	2	2
MAP4K4	2	2	2	2	2	2
MAP4K5	2	2	2	2	2	2
MAPK1	2	2	2	2	2	2
MAPK10	2	2	2	2	2	2
MAPK14	2	2	2	2	2	2
MAPK8	2	2	2	2	2	2
MAPK9	2	2	2	2	2	2
MAPKAPK2	2	2	2	2	2	2
MARK1	2	2	2	2	2	2
MCL1	2	2	2	2	2	2
MDM2	2	2	2	2	2	2
MDM4	2	2	2	2	2	2

MED12	2	2	2	2	2	2
MEF2B	2	2	2	2	2	2
MEN1	2	2	2	2	2	2
MERTK	2	2	2	2	2	2
MET	3.1	2.8	2	2	2	2
MITF	2	2	2	2	2	2
MKNK2	2	2	2	2	2	2
MLH1	2	2	2	2	2	2
MLL	2.62	2	2	2	2	2
MLL2	2	2	2	2	2	2
MLL3	3.1	2.7	2	2	2	2
MLL4	2	2	2	2	2	2
MPL	2	2	2	2	2	2
MRE11A	2	2	2	2	2	2
MS4A1	2.56	2	2	2	2	2
MSH2	2	2	2	2	2	2
MSH6	2	2	2	2	2	2
MTDH	2	2	3.52	3.28	2	2
MTHFR	2	2	2	2	2	2
MTOR	2	2	2	2	2	2
MTRR	2	2	4.34	4.5	2	2
MUTYH	2	2	2	2	2	2
MYC	2.64	2	4.42	4.06	2	2
MYCL1	2	2	2	2	2	2
MYCN	2	2	2	2	2	2
MYD88	2	2	2	2	2	2
NAT1	2	2	2	2	2	2
NAT2	2	2	2	2	2	2
NCAM1	2	2	2	2	2	2
NCF4	2	2	2	2	2	2
NCOA3	2	2	2	2	4.38	4.5
NCOR1	2	2	2	2	2	2
NEK11	2	2	2	2	2	2
NF1	2	2	2	2	2	2
NF2	2	2	2	2	2	2
NFE2L2	2	2	2	2	2	2
NFKBIA	2	2	2	2	2	2
NKX2-1	2	2	2	2	2	2
NOS3	2.94	2.68	2	2	2	2
NOTCH1	3.08	2.94	2	2	2	2
NOTCH2	2	2	2	2	2	2
NPM1	2	2	2	2	2	2
NQO1	2	2	2	2	2	2
NRAS	2	2	2	2	2	2
NTRK1	2.68	2	2	2	2	2
NTRK2	2.82	2.78	2	2	2	2
NTRK3	2	2	2	2	2	2
NUP93	2	2	2	2	2	2
PAK1	2.56	2	2	2	2	2

PAK3	2	2	2	2	2	2
PALB2	2	2	2	2	2	2
PARP1	2	2	2	2	2	2
PARP2	2	2	2	2	2	2
PAX5	2.96	3.14	2	2	2	2
PBRM1	2	2	2	2	2	2
PDCD1	2	2	2	2	2	2
PDGFRA	2	2	2	2	2	2
PDGFRB	2	2	2	2	2	2
PDK1	2	2	2	2	2	2
PHF6	2	2.8	2	2	2	2
PHKA2	2	2	2	2	2	2
PIGF	2	2	2	2	2	2
PIK3CA	2	2	2	2	2	2
PIK3CB	2	2	2	2	2	2
PIK3CG	2.96	3.06	2	2	2	2
PIK3R1	2	2	2	2	2	2
PIK3R2	2	2	2	2	2	2
PLK1	2	2	2	2	2	2
PPARD	2	2	2	2	2	2
PPP1R13L	2	2	2	2	2	2
PPP2R1A	2	2	2	2	2	2
PRDM1	2	2	2	2	2	2
PRDX4	2	2	2	2	2	2
PRKAA1	2	2	4.32	4.6	2	2
PRKAR1A	2	2	2	2	2	2
PRKCA	2	2	2	2	2	2
PRKCB	2	2	2	2	2	2
PRKCE	2	2	2	2	2	2
PRKCG	2	2	2	2	2	2
PRKDC	2	2	2	2	2	2
PRRT2	2	2	2	2	2	2
PTCH1	2.94	3.14	2	2	2	2
PTEN	2	2	2	2	2	2
PTK2	2	2	4.06	3.56	2	2
PTPN11	2	2	2	2	2	2
PTPRD	2	2	2	2	2	2
RAC2	2	2	2	2	2	2
RAD50	2	2	2	2	2	2
RAD51	2	2	2	2	2	2
RAF1	2	2	2	2	2	2
RB1	2	2	2	2	4.58	3.82
RET	2	2	2	2	2	2
RICTOR	2	2	4.18	4.32	2	2
RMDN2	2	2	2	2	2	2
RNF43	2	2	2	2	2	2
ROCK1	2	2	2	2	2	2
RON	2	2	2	2	2	2
ROS1	2	2	2	2	2	2

RPL13	2	2	2	2	2	2
RPS6KA1	2	2	2	2	2	2
RPS6KB1	2	2	2	2	2	2
RPTOR	2	2	2	2	2	2
RRM1	2	2	2	2	3.56	3.02
RUNX1	2	2	2	2	2	2
SDHA	2	2	2	2	2	2
SDHAF1	2	2	2	2	2	2
SDHAF2	2	2	2	2	2	2
SDHB	2	2	2	2	2	2
SDHC	2	2	2	2	2	2
SDHD	2	2	2	2	2	2
SETD2	2	2	2	2	2	2
SF3B1	2	2	2	2	2	2
SGK1	2	2	2	2	2	2
SHH	3.18	2.8	2	2	2	2
SIK1	2	2	2	2	2	2
SKP2	2	2	4.66	4.88	2	2
SLC10A2	2	2	2	2	6.16	4.84
SLC15A2	2	2	2	2	2	2
SLC22A1	2	2	2	2	2	2
SLC22A16	2	2	2	2	2	2
SLC22A2	2	2	2	2	2	2
SLC22A6	2	2	2	2	2	2
SLCO1B1	2	2	2	2	2	2
SLCO1B3	2	2	2	2	2	2
SMAD2	2	2	2	2	2	2
SMAD4	2	2	2	2	2	2
SMARCA4	2	2	2	2	2	2
SMARCB1	2	2	2	2	2	2
SMO	3.12	2.76	2	2	2	2
SOCS1	2	2	2	2	2	2
SOD2	2	2	2	2	2	2
SOX10	2	2	2	2	2	2
SOX2	2	2	2	2	2	2
SOX9	2	2	2	2	2	2
SPEN	2	2	2	2	2	2
SPG7	2	2	2	2	2	2
SPOP	2	2	2	2	2	2
SRC	2	2	2	2	4.5	5.04
SRD5A2	2	2	2	2	2	2
SRMS	2	2	2	2	5.28	5.12
STAG2	2	2	2	2	2	2
STAT1	2	2	2	2	2	2
STAT2	2	2	2	2	2	2
STAT3	2	2	2	2	2	2
STAT4	2	2	2	2	2	2
STAT5A	2	2	2	2	2	2
STAT5B	2	2	2	2	2	2

STAT6	2	2	2	2	2	2
STEAP1	2.78	2.5	2	2	2	2
STK11	2	2.54	2	2	2	2
STK3	2	2	3.68	3.32	2	2
STK4	2	2	2	2	5.2	5.08
SUFU	2	2	2	2	2	2
SULT1A1	2	2	2	2	2	2
SULT1A2	2	2	2	2	2	2
SULT1C4	2	2	2	2	2	2
SYK	3.08	3.12	2	2	2	2
TCF7L1	2	2	2	2	2	2
TCF7L2	2	2	2	2	2	2
TEK	2.9	3.02	2	2	2	2
TET2	2	2	2	2	2	2
TGFBR1	2.7	2.86	2	2	2	2
TGFBR2	2	2	2	2	2	2
TK1	2	2	2	2	2	2
TMPRSS2	2	2	2	2	2	2
TNF	2	2	2	2	2	2
TNFAIP3	2	2	2	2	2	2
TNFRSF10A	2	2	2	2	2	2
TNFRSF10B	2	2	2	2	2	2
TNFRSF14	2	2	2	2	2	2
TNFRSF8	2	2	2	2	2	2
TNFSF11	2	2	2	2	4.04	3.12
TNFSF13B	2	2	2	2	5.78	4.18
TOP1	2	2	2	2	5.72	5.38
TP53	2	2	2	2	2	2
TPMT	2	2	2	2	2	2
TPX2	2	2	2	2	4.46	5.16
TSC1	3.22	3.06	2	2	2	2
TSC2	2	2	2	2	2	2
TSHR	2	2	2	2	2	2
TYMS	2	2	2	2	2	2
TYRO3	2	2	2	2	2	2
U2AF1	2	2	2	2	2	2
UBE2I	2	2	2	2	2	2
UGT1A1	2	2	2	2	2	2
UGT1A9	2	2	2	2	2	2
UGT2B15	2	2	2	2	2	2
UGT2B17	2	2	2	2	2	2
UGT2B7	2	2	2	2	2	2
UMPS	2	2	2	2	2	2
VEGFA	2	2.84	2	2	2.8	3.38
VEGFB	2	2.54	2	2	2	2
VHL	2	2	2	2	2	2
WEE1	2	2	2	2	2	2
WISP3	2	2	2	2	2	2
WNK3	2	2	2	2	2	2

WT1	2	2	2	2	2	2
XPC	2	2	2	2	2	2
XPO1	2	2	2	2	2	2
XRCC1	2	2	2	2	2	2
XRCC4	2	2	2	2	2	2
YES1	2	2	2	2	2	2
ZAP70	2	2	2	2	2	2
ZC3HAV1	3.18	2.9	2	2	2	2
ZNF217	2	2	2	2	2	2
ZNF703	2	2	2	2	2	2

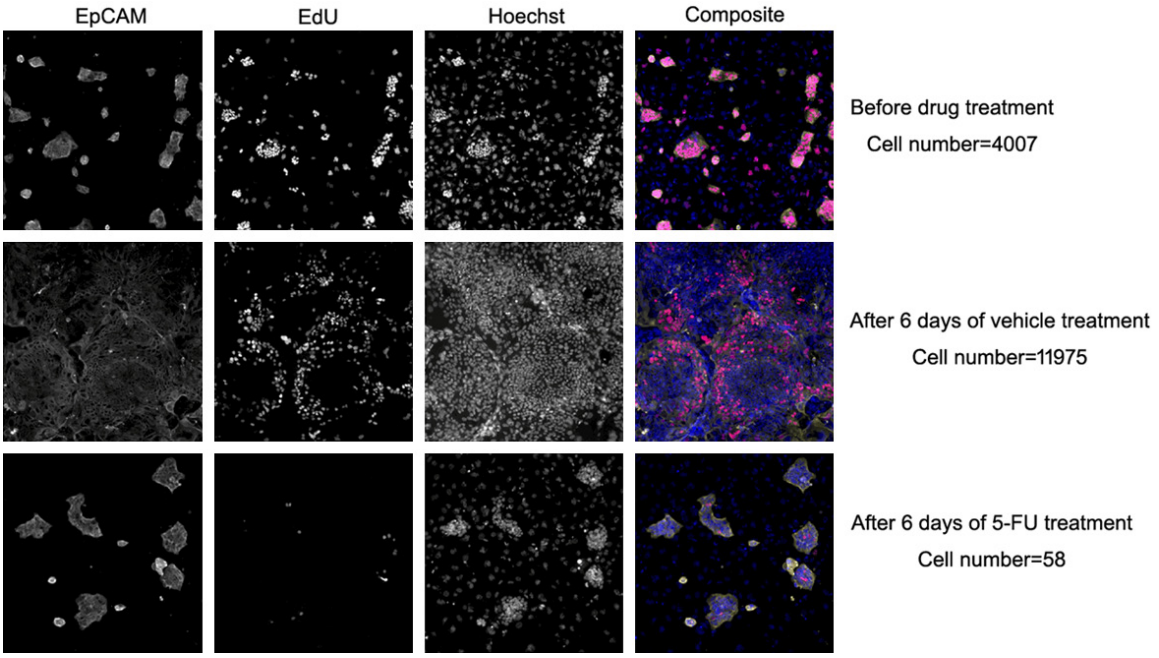

Figure S1. Drug effects with i-CR system. Epithelial cells marked with EpCAM monoclonal antibodies, newly synthesized DNA identified by EdU labeling, and cellular nuclei labeled with Hoechst dye. The first, second, and third rows showed i-CR cell numbers before drug treatment, after treatment with vehicle, and after treatment with 5-FU, respectively. Compared to cells treated by vehicle, most cells were killed by 5-FU. The cells were stained with EdU (red), EpCAM (yellow) and Hoechst (blue) in composite line.

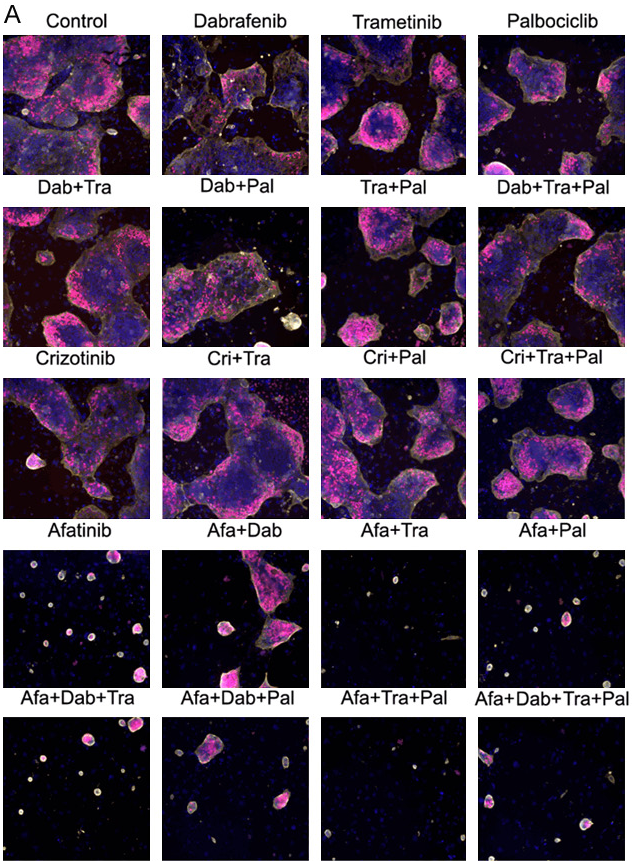

B

Drugs or regimens	EdU positive cell number	MI
Dabrafenib	6330	1.21
Trametinib	12757	0.60
Palbociclib	7959	0.97
Dabrafenib + Trametinib	7823	0.98
Dabrafenib + Palbociclib	8245	0.93
Trametinib + Palbociclib	11387	0.68
Dabrafenib + Trametinib + Palbociclib	9558	0.80
Crizotinib	5426	1.42
Crizotinib + Trametinib	11117	0.69
Crizotinib + Palbociclib	8440	0.91
Crizotinib + Trametinib + Palbociclib	11940	0.64
Afatinib	623	12.35
Afatinib + Dabrafenib	6140	1.25
Afatinib + Trametinib	47	164.47
Afatinib + Palbociclib	99	77.83
Afatinib + Dabrafenib + Trametinib	442	17.41
Afatinib + Dabrafenib + Palbociclib	1601	4.80
Afatinib + Trametinib + Palbociclib	10	794.34
Afatinib + Dabrafenib + Trametinib + Palbociclib	171	45.09

C

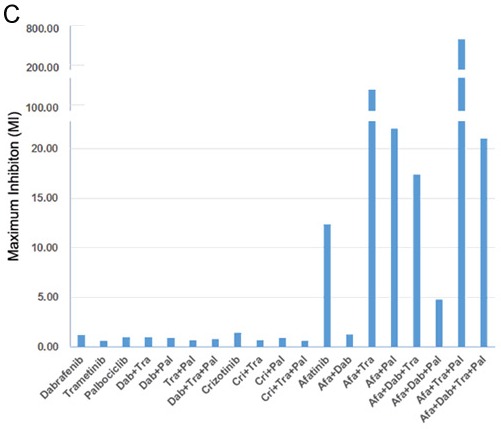

Figure S2. Representative data for high throughput screening with drug combinations *in vitro*. A. Image of cells treated with targeted drugs or drug combinations. Each microscopic frame represents a 0.976 mm × 0.976 mm view generated by the High-Content Screening (HCS) equipment. The cells were stained with EdU (red), EpCAM (yellow) and Hoechst (blue). B. Proliferating cells (EdU positive cells) and maximum inhibition (MI) after treatment of drugs or combination regimens. C. Bar graph of relationship between growth inhibition and treatment regimens. Dab, Tra, Pal, Cri, and Afa were the shortened forms of Dabrafenib, Trametinib, Palbociclib, Crizotinib, and Afatinib, respectively.

Table S3. Combination Index (CI) for pathways in i-CR cultures

No. of i-CR culture	Ei+Bi	Ei+Mi	Ei+Ci	E+c-METi	Bi+Mi	Bi+Ci	Mi+Ci
i-CR-1	1.99	0.53	0.23	0.98	1.02	1.01	1.06
i-CR-2	NA	0.24	0.32	1.00	NA	NA	1.15
i-CR-3	3.04	0.64	0.16	0.40	1.49	0.93	0.68
i-CR-4	4.71	1.13	0.10	0.97	2.11	1.82	1.97
i-CR-5	2.97	0.06	0.83	0.57	16.56	1.80	2.27
i-CR-6	1.56	0.68	0.15	0.83	1.01	0.98	0.95
i-CR-7	0.18	0.02	0.86	NA	0.82	0.96	1.15
i-CR-8	1.29	0.10	0.20	NA	1.66	1.48	0.84
i-CR-9	1.76	0.26	1.45	1.00	2.11	1.15	3.09
i-CR-10	2.81	0.33	0.06	0.72	1.18	1.56	2.53
i-CR-11	1.24	0.16	0.34	0.84	1.08	1.49	2.21
i-CR-12	1.98	0.33	0.03	0.60	1.00	1.03	1.27
i-CR-13	1.70	0.27	0.22	0.39	1.58	1.57	1.06

Note: Ei, EGFR inhibitor; Bi, BRAF inhibitor; Mi, MEK inhibitor; Ci, CDK4/6 inhibitor; c-METi, c-MET inhibitor; NA, not available; CI < 1, synergistic; CI = 1, additive; CI > 1, antagonistic.

Table S4. Maximum Inhibition (MI) for combinations of different pathways in i-CR cultures

No. of i-CR culture	Ei+Bi	Ei+Mi	Ei+Ci	Ei+Bi+Mi	Ei+Bi+Ci	Ei+Mi+Ci	Ei+Bi+Mi+Ci
i-CR-1	3.34	123.96	30.18	58.82	19.99	309.74	172.72
i-CR-2	1.68	15.55	6.83	2.75	2.44	238.92	39.24
i-CR-3	11.63	5693.89	983.12	222.30	223.29	13918.39	9954.87
i-CR-4	2.15	2.69	10.25	4.46	7.07	214.47	279.07
i-CR-5	3.24	271.22	10.27	20.73	8.99	87.49	49.63
i-CR-6	24.67	192.60	447.43	111.37	219.84	447.00	447.00
i-CR-7	5.22	39.21	123.10	87.79	10.41	907.67	220.07
i-CR-8	21.85	451.43	1085.49	254.00	449.30	1085.00	1085.00
i-CR-9	4.57	115.97	8.60	21.49	15.83	107.09	80.15
i-CR-10	2.95	140.79	6.18	10.77	5.20	561.03	50.59
i-CR-11	3.44	7.86	49.45	6.80	28.37	174.98	229.54
i-CR-12	9.37	110.04	2.69	956.90	42.00	440.44	813.97
i-CR-13	2.77	65.15	32.23	21.23	9.95	239.78	124.20
i-CR-14	1.20	3.83	2.14	1.46	1.70	38.92	13.11
i-CR-15	7.78	55.34	1430.91	34.59	172.96	5015.73	5015.73
i-CR-16	8.74	64.88	194.75	39.67	144.94	2069.08	586.54
i-CR-17	9.20	55.93	1861.97	38.94	302.41	6871.00	6871.00
i-CR-18	7.45	84.80	143.21	16.96	36.64	1040.23	255.79

Note: Ei, EGFR inhibitor; Bi, BRAF inhibitor; Mi, MEK inhibitor; Ci, CDK4/6 inhibitor.

Table S5. Consistency between *in vitro* i-CR cultures and *in vivo* paired PDX models

No. of i-CR culture	MI						No. of PDX	TGI					
	Ei	Mi	Ci	Ei+Mi	Ei+Ci	Ei+Mi+Ci		Ei	Mi	Ci	Ei+Mi	Ei+Ci	Ei+Mi+Ci
i-CR-2	3	2	2	65	32	239	PDX-2	NA	NA	NA	44%	22%	71%
i-CR-3	0.1	3	3	42	6	1003	PDX-3	NA	NA	NA	43%	32%	72%
i-CR-4	13	1	1	39	123	908	PDX-4	74%	41%	39%	84%	78%	95%
i-CR-7	1	1	4	1	9	171	PDX-7	19%	39%	33%	51%	56%	73%
i-CR-9	7	NA	NA	115	8	106	PDX-9	41%	NA	NA	74%	81%	101%
i-CR-10	1.5	0.6	1.2	26.7	8.2	186.5	PDX-10	74%	41%	39%	84%	78%	95%
i-CR-13	1	1	3.3	9.1	8.1	79.2	PDX-13	-18%	61%	69%	NA	NA	100%

Note: Ei, EGFR inhibitor; Mi, MEK inhibitor; Ci, CDK4/6 inhibitor; MI, maximum inhibition; TGI, tumor growth inhibition; NA, not available.

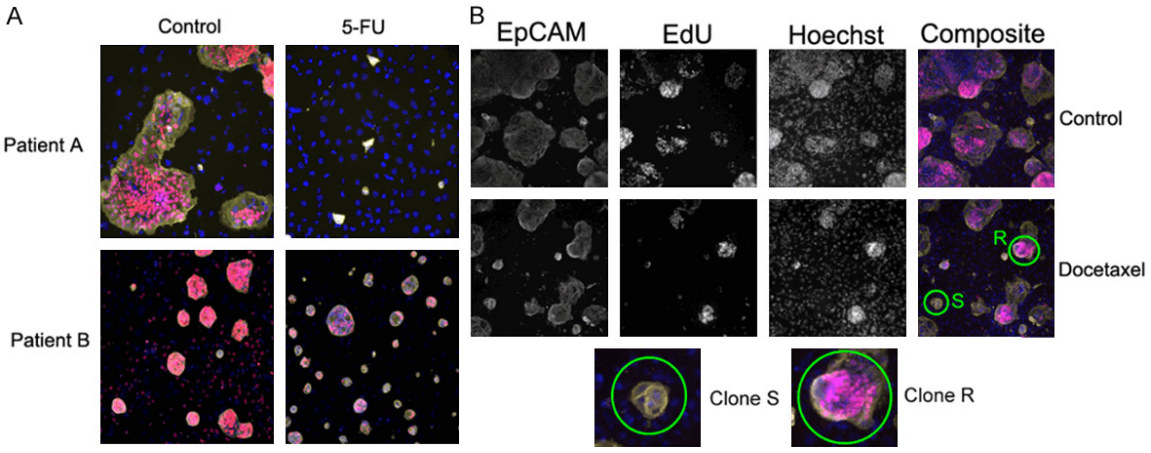

Figure S3. Utilization of i-CR system to study drug predictive biomarkers and resistance mechanisms. (A) Application of i-CR system to understand patient specific (patient A was sensitive to 5-FU, but patient B was not sensitive to 5-FU) and intra-tumor clonal (B) difference in the sensitivity to chemotherapeutic drugs. 5-FU and docetaxel were used to represent standard-of-care chemotherapeutic drugs. S denotes sensitive clones, R denotes drug resistant clones in the culture. Each microscopic frame represents a 0.976 mm × 0.976 mm view generated by the High-Content Screening (HCS) equipment.

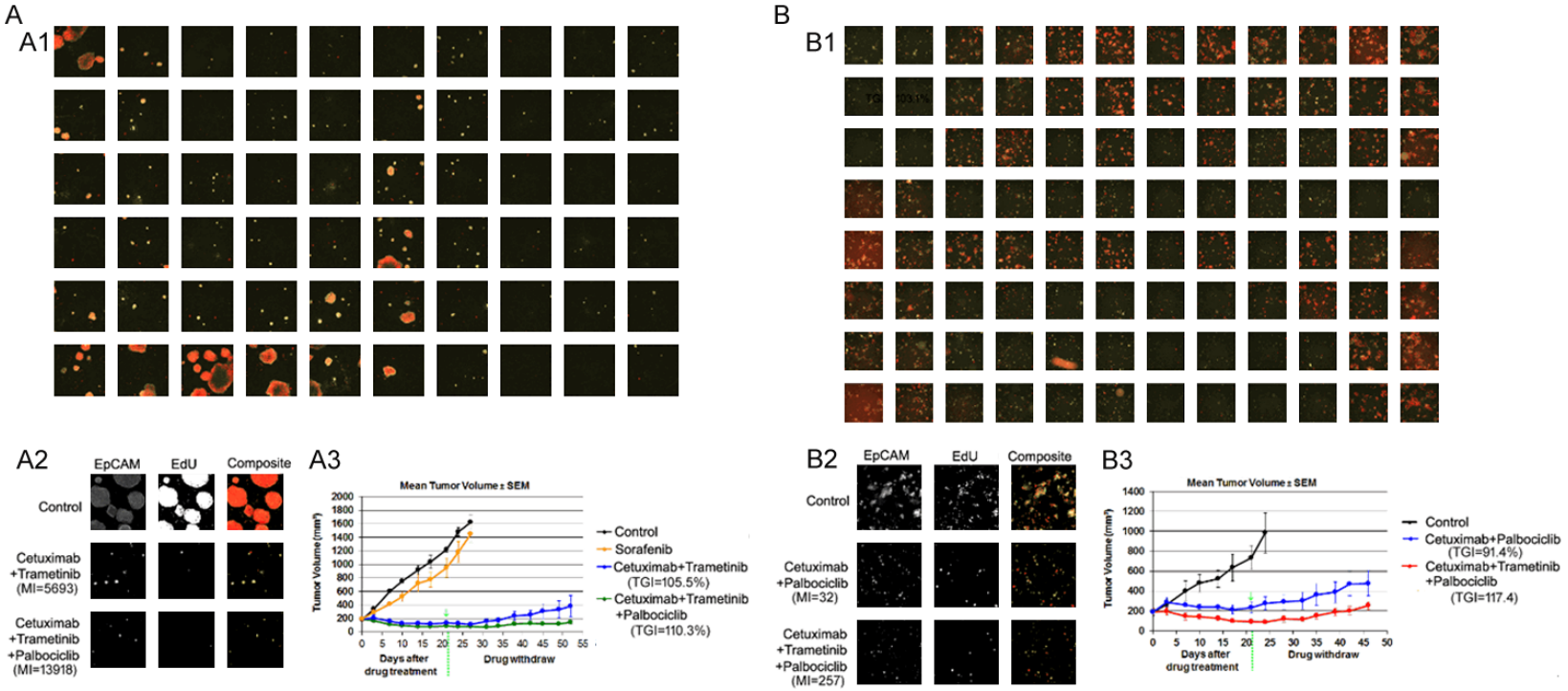

Figure S4. Potential applications of targeted drug combinations in other cancer types. (A) EGFR+MEK or EGFR+MEK+CDK4/6 inhibitors inhibited tumor growth of i-CR cells (A1, A2) and PDX models (A3) derived from one liver cancer patient. (B) EGFR+CDK4/6 or EGFR+MEK+CDK4/6 inhibitors inhibited tumor growth of i-CR cells (B1, B2) and PDX models (B3) derived from one gastric cancer patient. Each microscopic frame represents a 0.976 mm × 0.976 mm view generated by the High-Content Screening (HCS) equipment. The green arrow represented the time of drug withdraw.